
Calibration of Neural Networks

Ruslan Vasilev*

artnitolog@yandex.com

Alexander D'yakonov*

djakonov@mail.ru

Abstract

Neural networks solving real-world problems are often required not only to make accurate predictions but also to provide a confidence level in the forecast. The calibration of a model indicates how close the estimated confidence is to the true probability. This paper presents a survey of confidence calibration problems in the context of neural networks and provides an empirical comparison of calibration methods. We analyze problem statement, calibration definitions, and different approaches to evaluation: visualizations and scalar measures that estimate whether the model is well-calibrated. We review modern calibration techniques: based on post-processing or requiring changes in training. Empirical experiments cover various datasets and models, comparing calibration methods according to different criteria.

arXiv:2303.10761v1 [cs.NE] 19 Mar 2023

*Work done in 2020–2021 at Lomonosov Moscow State University as Ruslan Vasilev coursework (3rd year) supervised by Alexander D'yakonov.

Contents

1	Introduction	2
2	Problem Statement	2
3	Calibration Evaluation	3
3.1	Visualization	3
3.2	Calibration Metrics	4
4	Calibration Methods	6
4.1	Post-processing	6
4.1.1	Histogram Binning	6
4.1.2	Isotonic Regression	7
4.1.3	Generalizations of Platt Calibration	7
4.2	Calibration During Training	8
4.2.1	Label Smoothing	8
4.2.2	Focal Loss	9
5	Empirical Experiments	9
5.1	Experimental Design	9
5.2	Experiment Results	10
6	Conclusion	12
	References	14
	Appendices	16
A	Classification Accuracy	16
B	Binning-based Metrics	18
C	Proper Scoring Rules	24

1 Introduction

Deep learning is finding more and more applications in various fields. Neural networks are actively used in clinical practice [1], self-driving cars [2], machine translation [3], and other diverse applications.

Oftentimes, real-world problems require models that produce not only correct prediction but also a reliable measure of confidence in it. *Confidence* refers to probability estimate that the forecast is correct. For example, if an algorithm predicts a given sample of patients are healthy with confidence 0.9, we expect that 90% of them are really healthy. A model with reliable confidence estimation is called *calibrated*. Along with the interpretation of neural network predictions, confidence calibration is important when probability estimates are fed into subsequent algorithm steps (for example, language models decoding strategies [4]).

Modern neural networks often turn out to be poorly calibrated [5]. However, many other machine learning algorithms also produce biased confidence estimates [6, 7]. Various calibration techniques have been proposed for “classical” machine learning, some of which have been developed in deep learning.

2 Problem Statement

Consider a classification problem for objects from set \mathcal{X} with classes $\mathcal{Y} = \{1, \dots, K\}$. Suppose we have trained a *model* — an algorithm which produces vector of scores (*confidences*) $\mathbf{a}(x) = (a_1(x), \dots, a_K(x))$, $\sum_{j=1}^K a_j(x) = 1$, for each $x \in \mathcal{X}$. Next, the class corresponding to the highest confidence is assigned to the object:

$$\hat{y}(x) := \operatorname{argmax}_{j \in \mathcal{Y}} a_j, \quad \hat{p}(x) := a_{\hat{y}}.$$

We would like to interpret estimator \hat{p} as the probability that the true label coincides with the predicted one. If the estimate is accurate enough, then the model is called *calibrated*. Formally, the definition of calibration (*perfect calibration* in [5]) can be written as follows:

$$\mathbb{P}(y = \hat{y} \mid \hat{p} = p) = p \quad \forall p \in [0, 1]. \quad (1)$$

There are stronger definitions of model calibration¹ than (1). For example, according to [8], the classifier is called calibrated (originally, *well-calibrated*) if

$$\mathbb{P}(y = j \mid a_j = p) = p \quad \forall j \in \mathcal{Y}, \quad \forall p \in [0, 1] \quad (2)$$

that means the assurances given for each class (not just the predicted one) are calibrated.

In the case of real-world data and models, we cannot directly check (1) and (2), so various calibration metrics come in handy as well as visualizations that are reviewed in [section 3](#).

¹It should be noted that the term *calibration* also often refers to *methods* which make model confidences accurate.

Section 4 describes calibration methods — techniques that make confidences more reliable. First, one can calibrate confidences afterwards, i.e. find a transformation that maps biased estimates to calibrated. There are different algorithms that find optimal transformations. Second, it is possible to apply special techniques during training, for example, loss function modifications.

Section 5 provides empirical comparison of calibration methods for modern neural network architectures and shows how the choice of loss function affects the calibration.

3 Calibration Evaluation

3.1 Visualization

Before defining calibration measures, we simplify the problem to binary classification: $\mathcal{Y} = \{0, 1\}$ — consider the model generates confidences \hat{p} that the object belongs to the positive class ($y = 1$). Binary classification is common in various applications and “classical” machine learning models: logistic regression, support vector machines, gradient boosted trees and others — the problem of their calibration were studied in [6, 7].

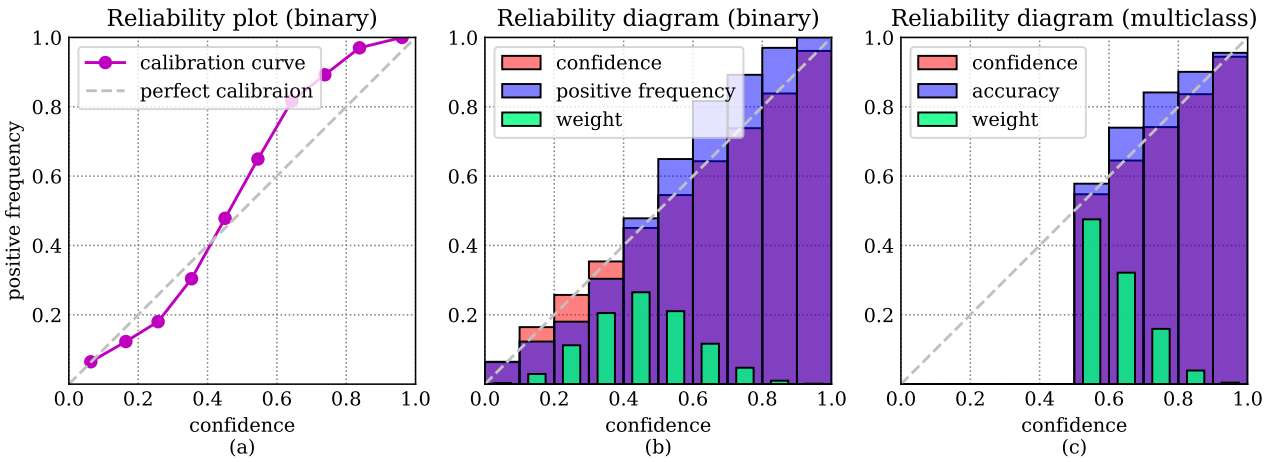


Figure 1: Options for visualizing confidence calibration. For clarity, synthetic data was generated. Support vector machine is used as a model (the distances to the separating hyperplane are scaled into $[0, 1]$).

Consider a set of objects (usually, another validation set), for each of which the true class is known and the confidence score is produced by the model. Divide the segment of all possible confidence values $[0, 1]$ into M equal-width intervals I_m :

$$I_1 = \left[0, \frac{1}{M}\right), I_2 = \left[\frac{1}{M}, \frac{2}{M}\right), \dots, I_{M-1} = \left[\frac{M-2}{M}, \frac{M-1}{M}\right), I_M = \left[\frac{M-1}{M}, 1\right]. \quad (3)$$

Thus, each confidence estimate falls into one of these intervals — let B_m denote the set of indices of those objects which confidences are in I_m . Both B_m and I_m are called *bins*.

For each bin B_m , we calculate positive frequency A_m^1 and average confidence C_m^1 :

$$A_m^1 = \frac{1}{|B_m|} \sum_{i \in B_m} \mathbb{1}(y_i = 1), \quad C_m^1 = \frac{1}{|B_m|} \sum_{i \in B_m} \hat{p}_i. \quad (4)$$

Finally, we can draw a plot $(C_m^1, A_m^1)_{m=1}^M$ which is called *reliability plot* [Figure 1 \(a\)](#). Also, the resulting curve is sometimes called *calibration curve*. The model is considered well-calibrated if its calibration curve is close to the diagonal (*in [subsection 3.2](#) we describe scalar metrics of such closeness*).

Likewise, $(C_m^1, A_m^1)_{m=1}^M$ can be depicted using a histogram, which is called *reliability diagram*. In [Figure 1 \(b\)](#) the average confidence is shown in red, and the positive frequency is shown in blue. If the red bar is higher than the blue one, then the algorithm underestimates confidences — *underconfidence*. The opposite case is called *overconfidence*. For better interpretation, the fraction of objects (bin *weight*) that fell into the bin can also be shown in the graph.

When the number of classes $n > 2$, reliability diagrams are built differently. The most popular approach corresponds to the definition [\(1\)](#). For each bin B_m , we estimate “accuracy” A_m and average confidence C_m :

$$A_m = \frac{1}{|B_m|} \sum_{i \in B_m} \mathbb{1}(y_i = \hat{y}_i), \quad C_m = \frac{1}{|B_m|} \sum_{i \in B_m} \hat{p}_i. \quad (5)$$

The difference between [\(4\)](#) and [\(5\)](#) is that in multiclass case \hat{y}_i and \hat{p}_i correspond to the estimated class and its confidence, while in binary case statistics are calculated only for a positive class.

Note that A_m and C_m estimate the left and the right of [\(1\)](#), respectively. They can be depicted on reliability diagram. For two classes, this approach is illustrated in [Figure 1 \(c\)](#). Bins to the left of 0.5 turn out to be empty because a binary classification algorithm assigns an object to a class that has confidence > 0.5 .

One can also consider classwise reliability diagrams [\[9\]](#). To make it, each class should be separately assigned to the positive, while all the others should be treated like the negative, so n reliability diagrams for the binary case can be built. Although the classwise approach is more informative [\(2\)](#), when the number of classes is large (for example, 1’000 or 22’000 in ImageNet [\[10\]](#)), it is usually impractical due to the interpretation difficulty. Therefore, reliability diagrams considering only the prediction confidence [\(5\)](#) are more common.

3.2 Calibration Metrics

In addition to visualizations, various metrics² can be used to evaluate the calibration of the model. One of the most common is Expected Calibration Error (ECE) [\[11\]](#). It estimates the expectation of the absolute difference between confidence and associated accuracy:

$$\mathbb{E}_{\hat{p}} |\mathbb{P}(y = \hat{y} \mid \hat{p}) - \hat{p}|. \quad (6)$$

²Here, *metric* refers to measure for the evaluation of algorithms

(6) can be approximated using the partition of the confidences into bins (l is the total number of objects in the considered set):

$$\begin{aligned}
\text{ECE} &= \sum_{m=1}^M \frac{|B_m|}{n} |A_m - C_m| \tag{7} \\
&= \sum_{m=1}^M \frac{|B_m|}{n} \left| \frac{1}{|B_m|} \sum_{i \in B_m} \mathbb{1}(y_i = \hat{y}_i) - \frac{1}{|B_m|} \sum_{i \in B_m} \hat{p}_i \right| \\
&= \frac{1}{n} \sum_{m=1}^M \left| \sum_{i \in B_m} \mathbb{1}(y_i = \hat{y}_i) - \sum_{i \in B_m} \hat{p}_i \right|.
\end{aligned}$$

Comparing (7) and reliability diagrams for a multiclass problem, we notice that ECE is exactly equal to the weighted average of the gaps between red and blue bars [Figure 1](#).

There are other metrics based on a partition of confidences into bins, although used less often. For example, one can calculate the maximum gap between confidence and accuracy [\[11\]](#):

$$\text{MCE} = \max_m |A_m - C_m|, \tag{8}$$

or take into account the confidence not only for the predicted class but also for all the others (classwise ECE) [\[9\]](#):

$$\text{cwECE} = \frac{1}{K} \sum_{j=1}^K \sum_{m=1}^M \frac{|B_m^j|}{n} |A_m^j - C_m^j|, \tag{9}$$

where B_m^j, A_m^j, C_m^j are, respectively, m -th bin, accuracy and confidence, if we consider j -th class positive, and collect all the others into negative. This metric corresponds to classwise reliability diagrams.

Instead of equal-width bins (3), bins with an equal number of samples can be used — sometimes confidence diagrams are built in this way. In [\[12\]](#), it was proposed to use equal-frequency bins to count the metrics described above. Further, an equal-width scheme will be considered. Also, in addition to l_1 -norm (i.e. averaging modules), we can use l_2 [\[13\]](#).

The problem with binning metrics is the dependence on the number of bins. An alternative approach is to use proper scoring rules. We consider Negative Log-Likelihood (NLL):

$$\text{NLL} = -\frac{1}{l} \sum_{i=1}^n \log a_{i,y_i} \tag{10}$$

where y_i is the true class label, a_{i,y_i} is a confidence of the algorithm in it, n is a total number of objects.

Another proper scoring rule, which can be used to evaluate model calibration, is Brier Score:

$$\text{BS} = \frac{1}{n} \sum_{i=1}^n \sum_{j=1}^K (a_{ij} - \mathbb{1}(y_i = j))^2, \tag{11}$$

where K is a number of classes.

4 Calibration Methods

There are two main types of calibration techniques. First, model outputs can be post-processed. Special transformation, *calibration map*, maps biased probability estimates to the calibrated ones. Second, calibration can be incorporated into the model training itself.

4.1 Post-processing

The transformation is usually found on a hold-out set (*calibration set*) $(x_i, y_i)_{i=1}^n$. It can be the same dataset used for hyperparameter tuning, but not the training set because model outputs distribution on training data is not the same as on unseen data.

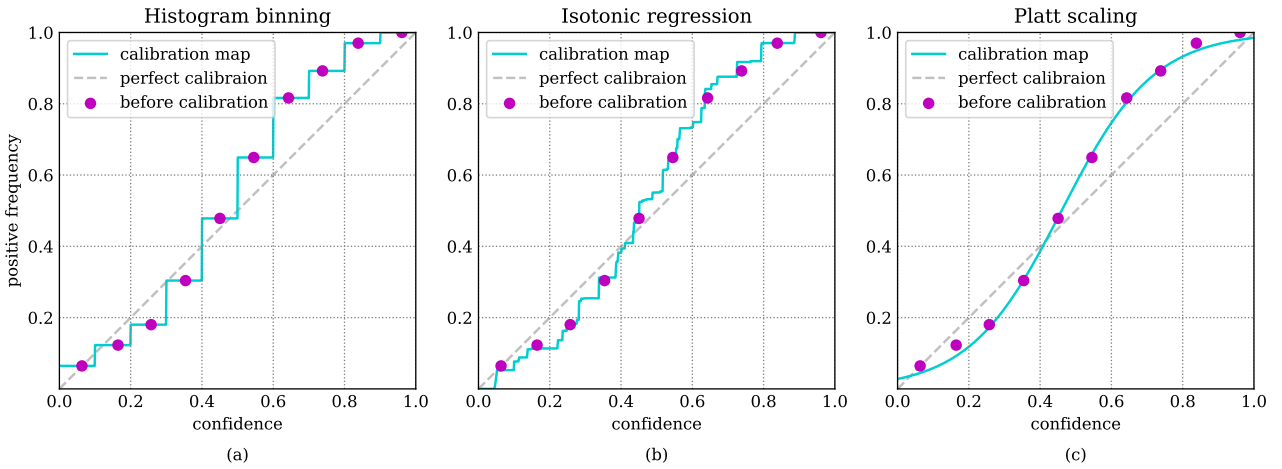


Figure 2: Different calibration maps for binary classification (the same data and model as in Figure 1).

4.1.1 Histogram Binning

The method was originally introduced in [14] to calibrate decision trees and naive Bayes classifiers. A calibration map in histogram binning is piecewise constant. Consider the binary case: the set of output confidence values is divided into bins B_1, \dots, B_M (usually equal-width (3) or equal-frequency), and scores that fall into B_m are replaced with the common θ_m . To find $\theta_1, \dots, \theta_M$, the following optimization problem is solved:

$$\sum_{m=1}^M \sum_{i \in B_m} (\theta_m - y_i)^2 \rightarrow \min_{\theta_1, \dots, \theta_M} . \quad (12)$$

In such a statement the optimal θ_m equals the fraction of positive objects that fall into B_m . The calibration map is illustrated in Figure 2 (a).

The method is generalized to the multiclass case using the strategy *one-vs-rest*: each class is separately declared positive and K piecewise constant functions are constructed. In the inference stage, a calibrated vector is additionally normalized.

4.1.2 Isotonic Regression

The method was proposed in [8]. For the binary case, the map is piecewise constant again, but both the number of the intervals M and their boundaries are optimized. The constraint is that the map should be non-decreasing. Thus, the following problem is solved:

$$\sum_{m=1}^M \sum_{i \in \tilde{B}_m} (\theta_m - y_i)^2 \rightarrow \min_{\substack{M \\ \theta_1 \leq \dots \leq \theta_M \\ 0 = \alpha_0 \leq \alpha_1 \leq \dots \leq \alpha_{M-1} \leq \alpha_M = 1}} \quad (13)$$

where $\tilde{B}_1 = \{i : \alpha_0 \leq \hat{p}_i < \alpha_1\}, \dots, \tilde{B}_m = \{i : \alpha_{m-1} \leq \hat{p}_i < \alpha_m\}$. The shape of the function is illustrated in Figure 2.

Isotonic regression is generalized to the multiclass case in the same way as histogram binning.

4.1.3 Generalizations of Platt Calibration

Originally, the method was proposed in [15] for calibration of the support vector machines. As can be seen in the illustrations Figure 1, Figure 2, if we rescale the distances $r(x)$ from the objects to the separating hyperplane into $[0, 1]$ and treat them as confidences in positive class, then the reliability plot will have the form of a sigmoid:

$$\hat{p}(x) = \frac{1}{1 + e^{-(\alpha r(x) + \beta)}}. \quad (14)$$

Scale parameter α and location parameter β are optimized on a calibration set using maximum likelihood estimation. In this method, the transformation is continuous and allows different generalizations to the multiclass case.

The last linear layer of a neural network for the object x outputs the logit vector: $\mathbf{z} = (z_1, \dots, z_K)$. To estimate class probabilities, the vector is transformed with softmax $\sigma(\cdot)$:

$$\sigma(\mathbf{z}) = \frac{1}{\sum_{j=1}^K \exp(z_j)} (\exp(z_1), \dots, \exp(z_K)),$$

so it is possible to generalize Platt Calibration by introducing scale and location parameters for logits:

$$a(x) = \sigma(\mathbf{W} \cdot \mathbf{z} + \mathbf{b}). \quad (15)$$

Parameters \mathbf{W} and \mathbf{b} are also optimized with maximum likelihood estimation on a calibration set, which is equivalent to minimizing NLL (10). Depending on \mathbf{W} and \mathbf{b} shapes, different generalization may be defined:

1. Temperature scaling:

$$\mathbf{W} = \frac{1}{T} \in \mathbb{R}, \quad T > 0, \quad \mathbf{b} = \mathbf{0}.$$

Generalization of Platt Calibration with a single scalar parameter. The method is one of the most frequently used. An increase in temperature T leads to an increase in uncertainty — an increase in the entropy of the output distribution. Decreasing T , on the contrary,

increases confidence in the predicted class. At the same time, the predicted class remains unchanged.

2. Vector scaling:

$$\mathbf{W} = \text{diag}(\mathbf{v}) \in \mathbb{R}^{K \times K} \text{ — diagonal matrix, } \mathbf{v} \in \mathbb{R}^K.$$

In this approach, a different scale factor is optimized for each class (and the bias, if $\mathbf{b} \neq \mathbf{0}$ is optimized too).

3. Matrix scaling:

$$\mathbf{W} \in \mathbb{R}^{K \times K}, \mathbf{b} \in \mathbb{R}^K.$$

Matrix scaling is the most general parametrization in this group of methods and is equivalent to logistic regression in the logit space. However, with a large number of classes, the method has too many parameters, which can lead to overfitting, because a calibration set is usually not large.

Note that to implement any of these methods, it is enough to add a linear layer (of the required dimension) to the frozen neural network.

4.2 Calibration During Training

The performance of neural networks strongly depends on the loss function. Usually, NLL (10) is used. Given an object x , it is equal to the cross-entropy between the true classification one-hot distribution \mathbf{y} and the predicted distribution:

$$\text{CE}(\mathbf{y}, \mathbf{a}) = - \sum_{j=1}^K y_j \log a_j. \quad (16)$$

To improve the calibration of the model, one can modify the loss function itself.

4.2.1 Label Smoothing

In this method, the degenerate distribution of the target is replaced by a smoothed one. The smoothing degree can be tuned using the parameter $\alpha \in [0, 1]$:

$$\mathbf{y} = (y_1, \dots, y_K) \mapsto \left((1 - \alpha)y_1 + \frac{\alpha}{K}, \dots, (1 - \alpha)y_K + \frac{\alpha}{K} \right) = \mathbf{y}'. \quad (17)$$

As parameter α increases, the distribution of \mathbf{y}' becomes more uniform. After this transformation, $\text{CE}(\mathbf{y}', \mathbf{a})$ the cross-entropy between the smoothed classification vector and the predicted distribution is minimized.

Although using of smoothed labels to train a classifier is not a new idea, this approach was proposed for calibration in [16].

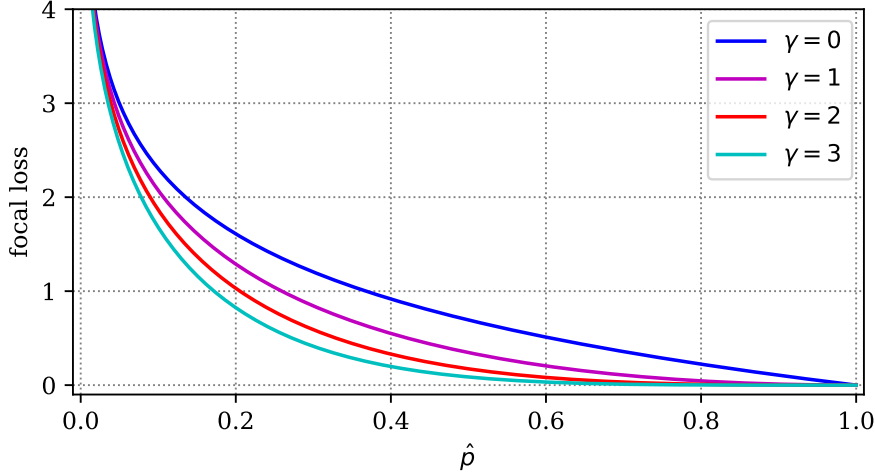


Figure 3: Focal loss on a single object. \hat{p} — probability estimation for a true class

4.2.2 Focal Loss

The focal loss was originally introduced to tackle the problem of class imbalance [17]. In terms of confidence calibration, the idea was first used in [18]. For an object belonging to the j -th class, the focal loss has the following definition:

$$\text{FL} = -(1 - a_j)^\gamma \cdot \log a_j, \quad \gamma \geq 0. \quad (18)$$

Note that the loss function becomes the cross-entropy when $\gamma = 0$. Increasing parameter γ , as we see in Figure 3, decreases the penalty for those objects with already high confidence in the true class. While the cross-entropy is the upper bound of the Kullback–Leibler divergence between the true \mathbf{y} and the predicted \mathbf{a} distribution, the focal error has the entropy of the predicted distribution $H(\mathbf{a})$ [18] subtracted from the estimate:

$$\text{CE}(\mathbf{y}, \mathbf{a}) \geq \text{KL}(\mathbf{y}||\mathbf{a}), \quad \text{FL}(\mathbf{y}, \mathbf{a}) \geq \text{KL}(\mathbf{y}||\mathbf{a}) - \gamma \cdot H(\mathbf{a}).$$

Thus, optimizing the focal error additionally increases the entropy of the predicted distribution and helps to tackle overconfidence.

5 Empirical Experiments

5.1 Experimental Design

The following datasets are used in the experiments:

- **CIFAR-10** [19]: The dataset consists of 60 000 color images 32×32 . *Training / validation / test* splits are respectively 50 000 / 5 000 / 5 000.
- **CIFAR-100** [19]: 60 000 color images 32×32 , 100 classes. *Training / validation / test*: 50 000 / 5 000 / 5 000.

- **ImageNet 2012** [10]: Large dataset with color images organized into 1000 classes. *Training / validation / test*: 1.2 m / 25 000 / 25 000.
- **Tiny ImageNet** [10]: 110 000 color images 64×64 , organized into 200 classes, subset of the previous dataset. *Training / validation / test*: 100 000 / 5 000 / 5 000.

Pre-trained neural networks with various architectures from open repositories were used for calculations. In experiments, models and datasets are divided into two main groups:

1. The first group includes neural networks trained on CIFAR-10, CIFAR-100, and ImageNet. The weights for the models are obtained respectively from the repositories [20, 21, 22]. Models from this group are used to compare calibration methods based on post-processing.
2. The second group includes pre-trained neural networks from the repository [23]. The datasets used here are CIFAR-10, CIFAR-100, and Tiny ImageNet. These neural networks were trained in [18] — focal error and label smoothing were used for the considered models.

The models were trained on the *training* data (*or its subset*), calibrated on the *validation* set — all diagrams and metrics correspond to the *test* set.

Code used in all experiments is published in [24]: temperature, vector, and matrix scaling are implemented using PyTorch, and other methods and evaluation are implemented with SciPY and scikit-learn. Histogram binning use 20 bins; ECE, cwECE, and MCE are calculated on 15 bins partition; reliability diagrams use 10 bins.

5.2 Experiment Results

Complete tables with measurements are given in [appendix](#), additional reliability diagrams for all the models considered in this work can be found in the accompanying repository [24].

Consider the reliability diagrams for ShuffleNetV2 (CIFAR-100, [Figure 4](#)): we see a “typical” state of modern neural networks calibration — overconfidence. Calibration methods help to correct the situation: in this case, temperature scaling works best for all the metrics. However, histogram binning changes probabilities too aggressively when the number of classes is large, as can be seen from the weights change.

For a small number of classes, on the contrary, histogram binning works best in terms of confidence in prediction ([Table 5](#), [Table 6](#) — for almost all models on CIFAR-10). Note that here neural networks already solve the classification problem with very high accuracy. Almost all probabilities of the predicted class are close to 1, as, for example, on [Figure 5](#). In terms of MCE ([Table 9](#), [Table 10](#)) — metric, that doesn’t consider weights of bins — histogram binning leads to low calibration.

For matrix scaling, we do not provide reliability diagrams: the method overfits too much when the number of classes is large. As a result, matrix scaling significantly degrades the classification quality ([Table 3](#), [Table 4](#)) for all datasets, except, again, the low-class CIFAR-10.

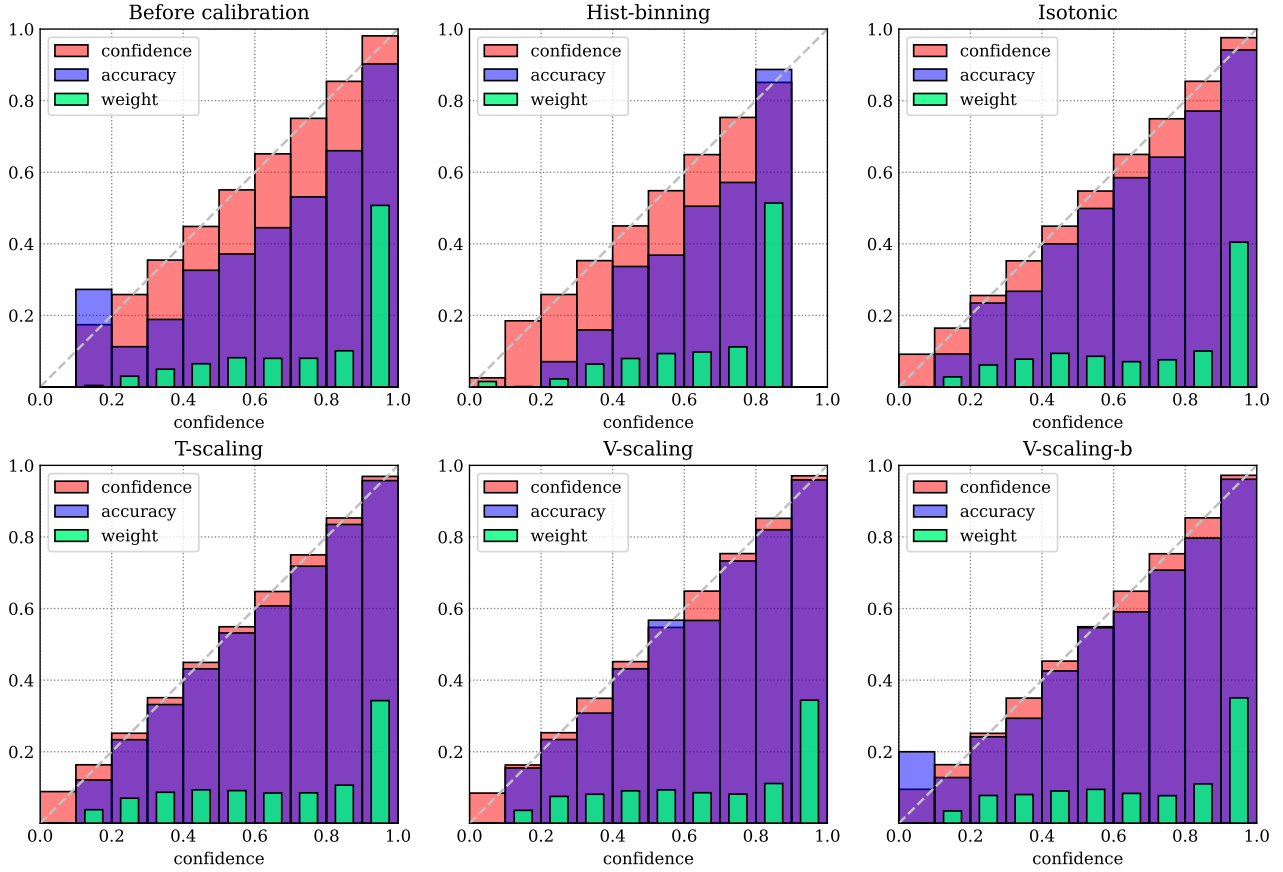


Figure 4: CIFAR-100, ShuffleNetV2_x0_5

One of the most common methods of neural network calibration is temperature scaling. The method doesn't affect classification predictions, while other calibration options almost always reduce accuracy (Table 3, Table 4).

In terms of NLL, temperature and vector scaling are the best as expected, because this loss was minimized during calibration: Table 11, Table 12. As for Brier Score, the best calibration method in many cases was isotonic regression: Table 13, Table 14.

Dataset	Model	CE	FL 1	FL 2	FL 3	LS 0.05
CIFAR-10	DenseNet121	4.53	3.47	2.02	1.68	1.65
CIFAR-10	ResNet110	4.73	3.70	2.78	1.61	2.20
CIFAR-10	ResNet50	4.26	3.88	2.55	1.58	3.07
CIFAR-10	Wide-ResNet-26-10	3.25	2.66	1.57	1.98	4.33
CIFAR-100	DenseNet121	20.90	14.54	8.40	4.49	13.27
CIFAR-100	ResNet110	19.76	15.35	12.10	9.22	11.44
CIFAR-100	ResNet50	18.14	13.36	8.60	4.99	8.15
CIFAR-100	Wide-ResNet-26-10	16.28	9.12	4.22	2.20	5.27
TinyImageNet	ResNet50	15.98	7.87	3.32	1.93	15.73

Table 1: ECE, % – Expected Calibration Error Error (lower is better), 15 bins without post-processing, columns correspond to different loss functions

Dataset	Model	CE	FL 1	FL 2	FL 3	LS 0.05
CIFAR-10	DenseNet121	0.948	0.755	0.514	0.524	0.576
CIFAR-10	ResNet110	0.990	0.804	0.660	0.505	0.673
CIFAR-10	ResNet50	0.941	0.836	0.625	0.524	0.766
CIFAR-10	Wide-ResNet-26-10	0.699	0.611	0.479	0.523	0.869
CIFAR-100	DenseNet121	0.458	0.364	0.280	0.254	0.315
CIFAR-100	ResNet110	0.433	0.372	0.321	0.281	0.299
CIFAR-100	ResNet50	0.412	0.337	0.282	0.256	0.271
CIFAR-100	Wide-ResNet-26-10	0.372	0.264	0.218	0.226	0.239
TinyImageNet	ResNet50	0.250	0.218	0.205	0.203	0.231

Table 2: cwECE, % – Classwise Expected Calibration Error (lower is better), 15 bins without post-processing, columns correspond to different loss functions

Focal loss and label smoothing result in better calibrated models than the ones optimizing the cross-entropy — both in terms of calibration in the predicted class (Table 1) and classwise

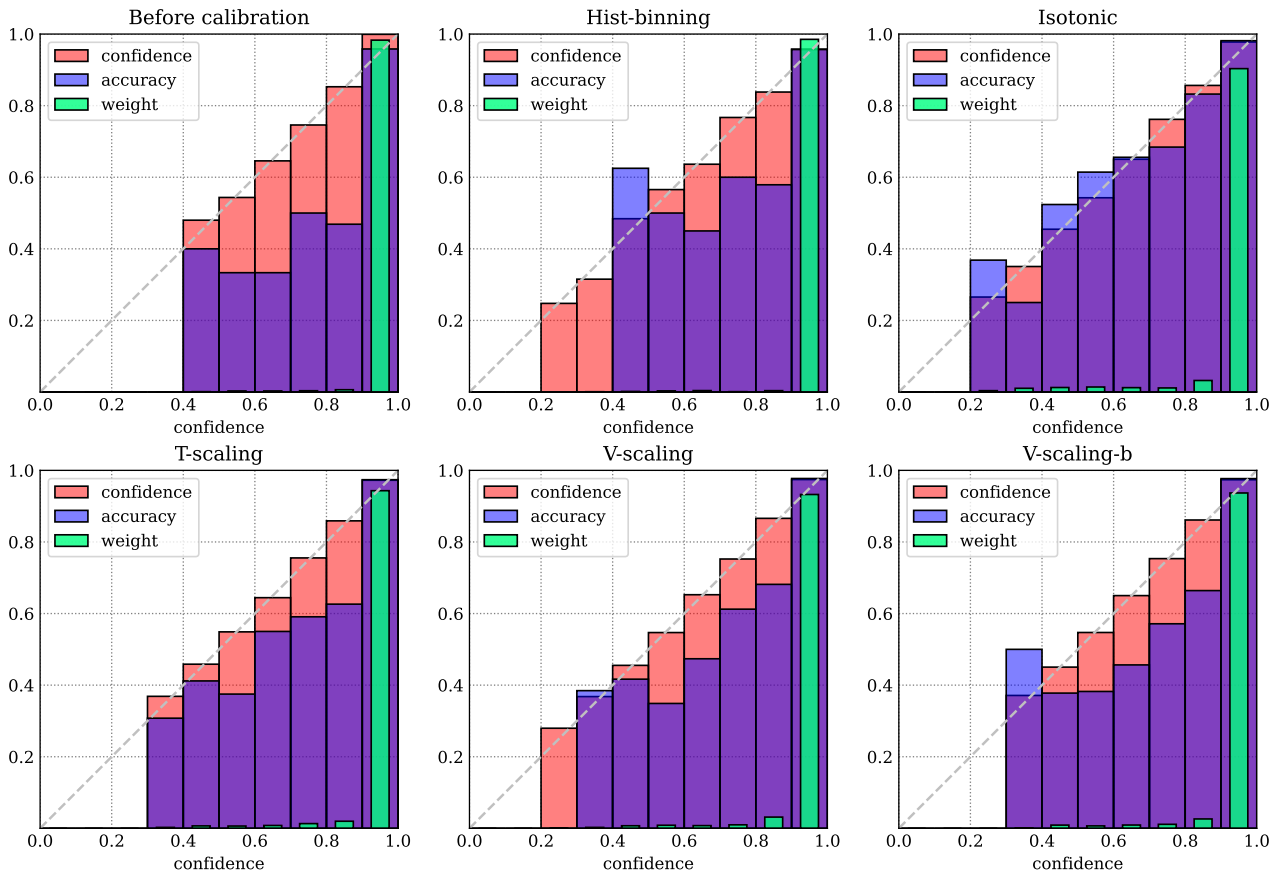


Figure 5: CIFAR-10, DenseNet121 (CE)

estimates (Table 2). At the same time, such models can be further calibrated with post-processing. In the original paper [18], temperature scaling was used to calibrate models trained with focal loss. Although this approach does show good results with respect to ECE (Table 6), vector scaling works better for classwise cwECE (Table 8). As for models of the first group (Table 7), vector scaling also basically minimizes cwECE. These results are quite expected since vector scaling finds separate coefficients for each class.

Consider also reliability diagrams for EfficientNet (Figure 6). Among all the models used, the underconfidence is most clearly visible in this neural network: most of the predictions fall not into $[0.9, 1]$, but into $[0.8, 0.9)$. The reason for this behavior may be training setup: the model was trained with label smoothing ($\alpha = 0.1$) [22]. All calibration methods resulted in a noticeable increase in the confidence of the answers.

6 Conclusion

In this work, the main methods of confidence calibration were compared on different neural network architectures, datasets, and criteria.

The applicability of a particular method depends significantly on the amount of data and the selected evaluation criterion. Algorithms, in which separate calibration maps are found for each class, work well only if there is a sufficient amount of data in the calibration set (this can usually be provided when the number of classes is small). Strategies based on linear

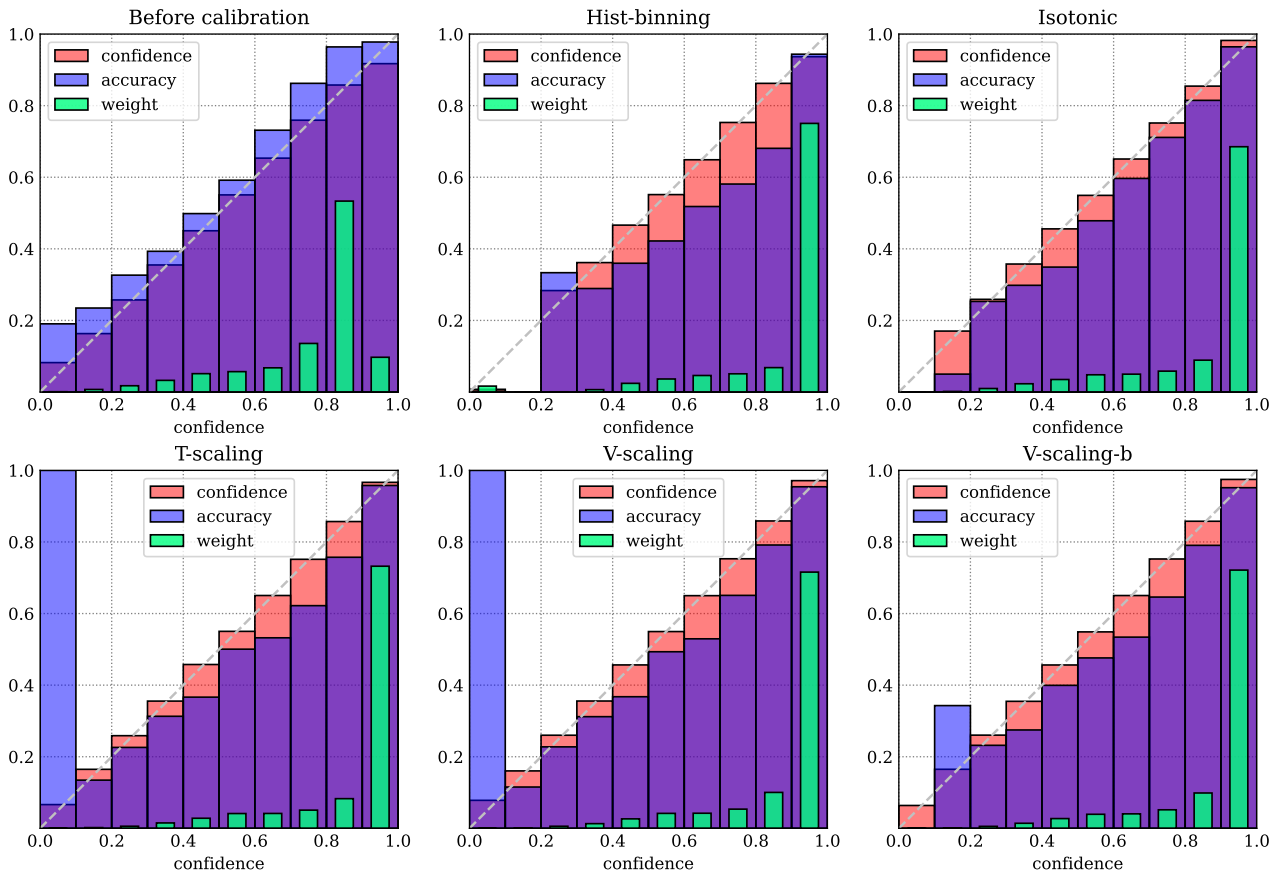


Figure 6: ImageNet, EfficientNet_b8

transformation of logits (for example, temperature scaling) show high quality in problems with a large number of classes but are subject to overfitting when parameterization is excessive (matrix scaling).

Confidence calibration is still open to further research in machine learning: as shown in this work, not only calibration methods but also criteria choice can lead to different results.

References

1. *Anwar S. M.* [et al.]. Medical image analysis using convolutional neural networks: a review // *Journal of medical systems*. — 2018. — Vol. 42, no. 11. — P. 1–13.
2. *Grigorescu S., Trasnea B., Cocias T., Macesanu G.* A survey of deep learning techniques for autonomous driving // *Journal of Field Robotics*. — 2020. — Vol. 37, no. 3. — P. 362–386.
3. *Wu Y.* [et al.]. Google’s neural machine translation system: Bridging the gap between human and machine translation // *arXiv preprint: 1609.08144*. — 2016.
4. *Holtzman A.* [et al.]. The curious case of neural text degeneration // *arXiv preprint arXiv:1904.09751*. — 2019.
5. *Guo C., Pleiss G., Sun Y., Weinberger K. Q.* On calibration of modern neural networks // *International Conference on Machine Learning*. — PMLR. 2017. — P. 1321–1330.
6. *Niculescu-Mizil A., Caruana R.* Predicting good probabilities with supervised learning // *Proceedings of the 22nd international conference on Machine learning*. — 2005. — P. 625–632.
7. *Caruana R., Niculescu-Mizil A.* An empirical comparison of supervised learning algorithms // *Proceedings of the 23rd international conference on Machine learning*. — 2006. — P. 161–168.
8. *Zadrozny B., Elkan C.* Transforming classifier scores into accurate multiclass probability estimates // *Proceedings of the eighth ACM SIGKDD international conference on Knowledge discovery and data mining*. — 2002. — P. 694–699.
9. *Kull M.* [et al.]. Beyond temperature scaling: Obtaining well-calibrated multi-class probabilities with Dirichlet calibration // *Advances in Neural Information Processing Systems*. Vol. 32 / ed. by H. Wallach [et al.]. — Curran Associates, Inc., 2019.
10. *Deng J.* [et al.]. Imagenet: A large-scale hierarchical image database // *2009 IEEE conference on computer vision and pattern recognition*. — Ieee. 2009. — P. 248–255.
11. *Naeini M. P., Cooper G., Hauskrecht M.* Obtaining well calibrated probabilities using bayesian binning // *Proceedings of the AAAI Conference on Artificial Intelligence*. Vol. 29. — 2015.
12. *Nixon J.* [et al.]. Measuring Calibration in Deep Learning // *arXiv preprint: 1904.01685*. — 2020.
13. *Kumar A., Liang P., Ma T.* Verified Uncertainty Calibration // *Advances in Neural Information Processing Systems (NeurIPS)*. — 2019.
14. *Zadrozny B., Elkan C.* Obtaining calibrated probability estimates from decision trees and naive bayesian classifiers // *Icml*. Vol. 1. — Citeseer. 2001. — P. 609–616.
15. *Platt J.* [et al.]. Probabilistic outputs for support vector machines and comparisons to regularized likelihood methods // *Vol. 10*. — Cambridge, MA, 1999. — P. 61–74.
16. *Müller R., Kornblith S., Hinton G.* When does label smoothing help? // *Vol. 10*. — 2019.

17. *Lin T.-Y.* [et al.]. Focal loss for dense object detection // Proceedings of the IEEE international conference on computer vision. — 2017. — P. 2980–2988.
18. *Mukhoti J.* [et al.]. Calibrating Deep Neural Networks using Focal Loss. — 2020.
19. *Krizhevsky A., Hinton G.* Learning multiple layers of features from tiny images // Master's thesis, Department of Computer Science, University of Toronto. — 2009.
20. *Phan H.* huyvnphan/PyTorch_CIFAR10. — Version v3.0.1. — 01/2021. — URL: <https://doi.org/10.5281/zenodo.4431043>.
21. *chenyaofu.* PyTorch CIFAR models. — 2021. — URL: <https://github.com/chenyaofu/pytorch-cifar-models>.
22. *Wightman R.* PyTorch Image Models. — 2019. — URL: <https://github.com/rwightman/pytorch-image-models>.
23. *Mukhoti J., Kulharia V.* Code for [18]. — URL: https://github.com/torrvision/focal_calibration.
24. *Vasilev R.* Calibration (accompanying repository). — URL: <https://github.com/artnitolog/calibration>.

Appendices

A Classification Accuracy

Dataset	Model	Before calibration	Hist-binning	Isotonic	T-scaling	V-scaling	V-scaling-b	M-scaling-b
CIFAR-10	DenseNet121	93.92	93.52	93.72	93.92	93.84	93.80	93.80
CIFAR-10	DenseNet161	93.70	93.74	93.58	93.70	93.72	93.74	93.52
CIFAR-10	DenseNet169	94.08	93.44	93.84	94.08	94.02	93.94	93.78
CIFAR-10	GoogleNet	92.92	92.58	92.68	92.92	92.90	92.84	92.76
CIFAR-10	InceptionV3	93.32	93.12	93.28	93.32	93.22	93.32	93.26
CIFAR-10	MobileNetV2	93.42	93.40	93.42	93.42	93.26	93.36	93.36
CIFAR-10	ResNet18	92.54	92.14	92.34	92.54	92.48	92.40	92.18
CIFAR-10	ResNet34	93.24	92.74	92.92	93.24	93.14	93.16	92.94
CIFAR-10	ResNet50	93.44	93.10	93.22	93.44	93.40	93.38	93.24
CIFAR-10	VGG11_bn	91.96	91.66	91.84	91.96	91.86	91.80	91.98
CIFAR-10	VGG13_bn	93.86	93.40	93.74	93.86	93.92	93.82	93.68
CIFAR-10	VGG16_bn	93.52	93.38	93.42	93.52	93.36	93.36	93.36
CIFAR-10	VGG19_bn	93.76	93.36	93.62	93.76	93.70	93.84	93.56
CIFAR-100	MobileNetV2_x0_5	70.32	67.56	69.86	70.32	70.26	69.94	55.38
CIFAR-100	MobileNetV2_x1_0	73.34	70.74	72.98	73.34	73.20	73.50	59.24
CIFAR-100	MobileNetV2_x1_4	76.22	72.96	75.58	76.22	75.72	75.80	63.10
CIFAR-100	ResNet20	67.80	63.80	66.72	67.80	67.36	67.54	49.94
CIFAR-100	ResNet32	69.10	65.90	68.64	69.10	68.90	68.70	52.20
CIFAR-100	ResNet44	70.82	67.86	70.22	70.82	70.42	70.56	55.16
CIFAR-100	ResNet56	72.04	69.54	71.62	72.04	71.72	71.58	56.34
CIFAR-100	ShuffleNetV2_x0_5	66.86	64.22	66.68	66.86	66.98	66.58	50.02
CIFAR-100	ShuffleNetV2_x1_0	71.58	69.16	71.24	71.58	71.26	71.30	57.50
CIFAR-100	ShuffleNetV2_x1_5	73.60	70.90	73.34	73.60	73.72	73.80	61.30
CIFAR-100	ShuffleNetV2_x2_0	74.92	72.30	74.44	74.92	74.84	74.82	63.04
CIFAR-100	VGG11_bn	69.96	67.76	69.34	69.96	69.56	69.58	59.90
CIFAR-100	VGG13_bn	73.90	71.84	73.02	73.90	73.56	73.36	62.58
CIFAR-100	VGG16_bn	73.30	71.34	72.78	73.30	72.96	72.94	64.28
CIFAR-100	VGG19_bn	73.14	71.78	72.76	73.14	73.00	72.82	63.78
ImageNet	EfficientNet_b8	85.52	83.43	84.92	85.52	85.54	85.47	79.12
ImageNet	MobileNetV2_120d	77.68	73.57	76.79	77.68	77.36	77.16	59.84
ImageNet	RepVGG_b3	80.57	77.68	79.89	80.57	80.22	80.17	66.38
ImageNet	VGG19_bn	74.35	70.47	73.72	74.35	73.92	73.62	54.06

Table 3: Accuracy % (higher is better) – fraction of correct predictions, group 1

Dataset	Model	Before calibration	Hist-binning	Isotonic	T-scaling	V-scaling	V-scaling-b	M-scaling-b
CIFAR-10	DenseNet121 (CE)	94.92	94.98	94.84	94.92	94.94	94.96	94.76
CIFAR-10	DenseNet121 (FL 1)	94.84	94.68	94.82	94.84	95.00	95.02	94.52
CIFAR-10	DenseNet121 (FL 2)	94.90	94.60	94.96	94.90	94.84	94.80	94.80
CIFAR-10	DenseNet121 (FL 3)	94.24	94.24	94.20	94.24	94.34	94.24	94.36
CIFAR-10	DenseNet121 (LS 0.05)	94.52	94.62	94.66	94.52	94.56	94.58	94.62
CIFAR-10	ResNet110 (CE)	94.82	94.70	94.76	94.82	94.84	94.86	94.90
CIFAR-10	ResNet110 (FL 1)	94.80	94.90	94.84	94.80	94.86	95.00	94.98
CIFAR-10	ResNet110 (FL 2)	94.82	94.82	94.96	94.82	94.96	94.90	94.84
CIFAR-10	ResNet110 (FL 3)	94.70	94.64	94.84	94.70	94.84	94.86	94.70
CIFAR-10	ResNet110 (LS 0.05)	94.36	94.36	94.48	94.36	94.32	94.32	94.40
CIFAR-10	ResNet50 (CE)	95.02	94.62	94.66	95.02	95.00	94.96	94.82
CIFAR-10	ResNet50 (FL 1)	94.58	94.34	94.52	94.58	94.60	94.52	94.58
CIFAR-10	ResNet50 (FL 2)	94.80	94.62	94.82	94.80	94.90	94.90	94.88
CIFAR-10	ResNet50 (FL 3)	94.52	94.48	94.66	94.52	94.58	94.60	94.44
CIFAR-10	ResNet50 (LS 0.05)	94.26	94.02	94.18	94.26	94.26	94.16	94.30
CIFAR-10	Wide-ResNet-26-10 (CE)	96.12	96.02	96.08	96.12	96.20	96.20	96.10
CIFAR-10	Wide-ResNet-26-10 (FL 1)	95.70	95.26	95.56	95.70	95.64	95.66	95.70
CIFAR-10	Wide-ResNet-26-10 (FL 2)	95.56	95.06	95.50	95.56	95.40	95.46	95.48
CIFAR-10	Wide-ResNet-26-10 (FL 3)	95.64	95.62	95.80	95.64	95.74	95.74	95.64
CIFAR-10	Wide-ResNet-26-10 (LS 0.05)	95.66	95.50	95.40	95.66	95.64	95.68	95.42
CIFAR-100	DenseNet121 (CE)	75.32	74.52	75.26	75.32	75.76	75.70	65.60
CIFAR-100	DenseNet121 (FL 1)	75.66	74.12	75.90	75.66	76.02	76.00	65.24
CIFAR-100	DenseNet121 (FL 2)	75.90	73.50	76.22	75.90	75.90	76.02	65.32
CIFAR-100	DenseNet121 (FL 3)	76.10	72.90	75.86	76.10	76.16	76.20	65.06
CIFAR-100	DenseNet121 (LS 0.05)	75.54	74.56	75.66	75.54	75.66	75.74	66.60
CIFAR-100	ResNet110 (CE)	76.44	76.02	76.50	76.44	76.80	76.88	66.20
CIFAR-100	ResNet110 (FL 1)	76.84	75.28	76.48	76.84	77.34	77.28	66.52
CIFAR-100	ResNet110 (FL 2)	76.74	74.48	76.68	76.74	77.04	76.90	67.00
CIFAR-100	ResNet110 (FL 3)	76.30	74.80	76.56	76.30	76.66	76.82	66.46
CIFAR-100	ResNet110 (LS 0.05)	75.96	74.48	75.68	75.96	76.10	76.18	66.66
CIFAR-100	ResNet50 (CE)	76.00	74.48	75.62	76.00	76.12	76.14	65.86
CIFAR-100	ResNet50 (FL 1)	76.38	74.22	76.36	76.38	76.66	76.46	66.32
CIFAR-100	ResNet50 (FL 2)	76.58	73.90	76.10	76.58	76.52	76.46	65.40
CIFAR-100	ResNet50 (FL 3)	77.08	74.44	76.42	77.08	76.86	76.94	64.62
CIFAR-100	ResNet50 (LS 0.05)	76.18	74.38	76.24	76.18	76.42	76.48	67.98
CIFAR-100	Wide-ResNet-26-10 (CE)	78.26	77.22	77.98	78.26	78.38	78.22	67.72
CIFAR-100	Wide-ResNet-26-10 (FL 1)	79.84	78.10	79.80	79.84	79.76	79.76	68.82
CIFAR-100	Wide-ResNet-26-10 (FL 2)	79.64	77.54	79.64	79.64	79.96	80.04	69.44
CIFAR-100	Wide-ResNet-26-10 (FL 3)	79.70	76.96	79.62	79.70	79.86	79.80	70.18
CIFAR-100	Wide-ResNet-26-10 (LS 0.05)	78.14	75.98	77.90	78.14	78.26	78.24	69.62
TinyImageNet	ResNet50 (CE)	49.98	44.92	49.10	49.98	49.44	49.24	32.66
TinyImageNet	ResNet50 (FL 1)	50.10	44.96	49.48	50.10	50.04	49.94	31.32
TinyImageNet	ResNet50 (FL 2)	51.86	46.56	51.14	51.86	51.82	51.62	31.96
TinyImageNet	ResNet50 (FL 3)	51.06	44.56	50.18	51.06	50.82	50.94	32.08
TinyImageNet	ResNet50 (LS 0.05)	53.62	47.18	51.94	53.62	52.84	52.78	36.82

Table 4: Accuracy % (higher is better) – fraction of correct predictions, group 2

B Binning-based Metrics

Dataset	Model	Before calibration	Hist-binning	Isotonic	T-scaling	V-scaling	V-scaling-b	M-scaling-b
CIFAR-10	DenseNet121	1.86	1.08	2.10	1.64	1.67	1.58	1.49
CIFAR-10	DenseNet161	2.11	1.08	1.64	1.68	1.87	1.75	1.75
CIFAR-10	DenseNet169	2.04	1.42	1.87	1.72	1.64	1.62	1.64
CIFAR-10	GoogLeNet	1.65	0.89	1.36	1.21	1.46	1.37	1.34
CIFAR-10	InceptionV3	2.06	1.35	1.91	1.88	1.99	1.91	1.86
CIFAR-10	MobileNetV2	2.92	1.45	1.74	1.87	2.09	1.95	1.78
CIFAR-10	ResNet18	2.51	1.60	2.03	2.13	1.98	1.93	2.16
CIFAR-10	ResNet34	2.67	1.44	2.09	1.96	1.70	1.88	1.75
CIFAR-10	ResNet50	2.50	1.06	1.70	1.67	1.72	1.59	1.62
CIFAR-10	VGG11_bn	1.87	2.21	1.65	1.83	1.88	1.90	1.76
CIFAR-10	VGG13_bn	1.41	1.42	1.54	1.44	1.44	1.43	1.72
CIFAR-10	VGG16_bn	1.86	1.08	1.61	1.71	1.93	1.81	1.74
CIFAR-10	VGG19_bn	2.15	1.02	1.34	1.87	2.00	1.98	2.14
CIFAR-100	MobileNetV2_x0_5	12.69	9.39	5.86	3.28	3.31	3.57	44.57
CIFAR-100	MobileNetV2_x1_0	11.77	10.13	6.02	3.78	3.46	3.69	40.68
CIFAR-100	MobileNetV2_x1_4	9.66	10.13	4.29	2.90	2.69	2.86	36.79
CIFAR-100	ResNet20	11.21	9.01	5.79	2.48	3.11	3.13	50.05
CIFAR-100	ResNet32	13.95	10.34	5.47	2.61	2.28	2.77	47.79
CIFAR-100	ResNet44	14.99	8.42	6.42	3.18	3.49	3.48	44.84
CIFAR-100	ResNet56	14.72	7.86	5.68	3.13	3.10	3.40	43.65
CIFAR-100	ShuffleNetV2_x0_5	12.93	9.62	5.38	2.22	2.38	2.80	49.77
CIFAR-100	ShuffleNetV2_x1_0	11.68	8.15	5.90	3.68	4.24	4.18	42.32
CIFAR-100	ShuffleNetV2_x1_5	9.86	8.94	5.44	4.56	4.88	4.64	38.44
CIFAR-100	ShuffleNetV2_x2_0	7.68	10.14	4.91	4.26	4.78	4.78	36.80
CIFAR-100	VGG11_bn	15.86	10.61	7.78	5.17	5.80	6.08	29.38
CIFAR-100	VGG13_bn	14.06	8.12	7.19	5.84	5.80	5.84	27.53
CIFAR-100	VGG16_bn	19.33	8.87	5.74	4.18	3.93	4.03	28.60
CIFAR-100	VGG19_bn	20.17	8.79	5.22	4.53	3.74	3.61	31.98
ImageNet	EfficientNet_b8	8.98	4.88	2.96	3.17	3.51	3.95	20.15
ImageNet	MobileNetV2_120d	6.85	7.02	1.96	1.61	2.11	2.90	38.18
ImageNet	RepVGG_b3	3.23	6.17	3.61	3.95	4.08	4.76	32.42
ImageNet	VGG19_bn	3.69	9.26	3.93	1.92	1.53	2.16	44.68

Table 5: ECE % – Expected Calibration Error (lower is better), 15 bins, group 1

Dataset	Model	Before calibration	Hist-binning	Isotonic	T-scaling	V-scaling	V-scaling-b	M-scaling-b
CIFAR-10	DenseNet121 (CE)	4.53	0.38	1.24	1.64	1.19	1.29	1.45
CIFAR-10	DenseNet121 (FL 1)	3.47	0.87	0.65	1.26	0.88	1.05	1.44
CIFAR-10	DenseNet121 (FL 2)	2.02	0.97	0.73	0.95	1.08	1.01	1.18
CIFAR-10	DenseNet121 (FL 3)	1.68	1.17	1.32	1.49	1.32	1.38	1.84
CIFAR-10	DenseNet121 (LS 0.05)	1.65	0.93	1.55	1.22	1.28	1.24	1.29
CIFAR-10	ResNet110 (CE)	4.73	1.01	1.11	1.23	1.36	1.39	1.25
CIFAR-10	ResNet110 (FL 1)	3.70	0.71	0.99	1.11	1.20	1.06	1.05
CIFAR-10	ResNet110 (FL 2)	2.78	0.55	1.20	1.03	0.94	0.96	1.07
CIFAR-10	ResNet110 (FL 3)	1.61	0.84	0.96	1.24	0.94	0.84	1.01
CIFAR-10	ResNet110 (LS 0.05)	2.20	1.77	0.90	1.56	1.07	0.88	0.72
CIFAR-10	ResNet50 (CE)	4.26	0.70	0.96	1.41	1.17	1.10	1.23
CIFAR-10	ResNet50 (FL 1)	3.88	1.88	1.46	1.58	1.65	1.67	1.85
CIFAR-10	ResNet50 (FL 2)	2.55	1.08	1.09	1.17	1.52	1.52	1.14
CIFAR-10	ResNet50 (FL 3)	1.58	0.78	0.98	1.11	1.16	1.01	1.56
CIFAR-10	ResNet50 (LS 0.05)	3.07	1.23	1.14	1.35	1.35	1.43	1.40
CIFAR-10	Wide-ResNet-26-10 (CE)	3.25	0.60	0.50	1.07	0.84	0.91	0.90
CIFAR-10	Wide-ResNet-26-10 (FL 1)	2.66	0.95	1.03	0.87	1.08	1.17	1.05
CIFAR-10	Wide-ResNet-26-10 (FL 2)	1.57	1.40	1.12	1.18	1.37	1.31	1.42
CIFAR-10	Wide-ResNet-26-10 (FL 3)	1.98	0.82	0.89	1.06	1.08	0.86	0.89
CIFAR-10	Wide-ResNet-26-10 (LS 0.05)	4.33	0.72	0.94	0.99	1.17	1.17	1.23
CIFAR-100	DenseNet121 (CE)	20.90	7.00	6.18	4.82	4.74	4.72	34.38
CIFAR-100	DenseNet121 (FL 1)	14.54	6.03	7.31	5.18	5.22	5.38	34.71
CIFAR-100	DenseNet121 (FL 2)	8.40	10.42	4.47	4.16	4.37	4.42	34.63
CIFAR-100	DenseNet121 (FL 3)	4.49	9.10	4.16	3.98	4.55	4.45	34.84
CIFAR-100	DenseNet121 (LS 0.05)	13.27	6.98	7.03	7.44	3.32	3.49	33.31
CIFAR-100	ResNet110 (CE)	19.76	3.99	6.09	5.63	5.37	5.44	33.74
CIFAR-100	ResNet110 (FL 1)	15.35	6.16	6.56	4.87	4.83	4.84	33.41
CIFAR-100	ResNet110 (FL 2)	12.10	8.50	5.92	5.48	5.51	5.61	32.91
CIFAR-100	ResNet110 (FL 3)	9.22	8.68	4.67	5.36	5.41	5.39	33.53
CIFAR-100	ResNet110 (LS 0.05)	11.44	6.95	5.86	4.41	4.50	4.66	33.25
CIFAR-100	ResNet50 (CE)	18.14	4.75	7.24	6.02	6.52	6.53	34.07
CIFAR-100	ResNet50 (FL 1)	13.36	5.81	7.06	5.29	5.44	5.61	33.62
CIFAR-100	ResNet50 (FL 2)	8.60	9.41	4.90	4.72	4.91	4.90	34.52
CIFAR-100	ResNet50 (FL 3)	4.99	7.73	4.07	3.39	3.83	3.98	35.30
CIFAR-100	ResNet50 (LS 0.05)	8.15	7.68	6.61	5.27	5.32	5.32	31.94
CIFAR-100	Wide-ResNet-26-10 (CE)	16.28	4.91	6.43	4.79	5.21	5.00	32.23
CIFAR-100	Wide-ResNet-26-10 (FL 1)	9.12	8.12	5.40	4.31	4.35	4.24	31.16
CIFAR-100	Wide-ResNet-26-10 (FL 2)	4.22	7.61	3.47	3.87	4.01	3.75	30.53
CIFAR-100	Wide-ResNet-26-10 (FL 3)	2.20	8.05	3.33	3.62	3.62	3.79	29.80
CIFAR-100	Wide-ResNet-26-10 (LS 0.05)	5.27	7.52	5.36	4.78	4.85	4.83	30.37
TinyImageNet	ResNet50 (CE)	15.98	9.96	10.06	6.67	7.26	7.83	65.77
TinyImageNet	ResNet50 (FL 1)	7.87	9.96	6.12	4.17	4.76	5.54	67.23
TinyImageNet	ResNet50 (FL 2)	3.32	9.49	4.94	2.98	3.63	3.82	66.81
TinyImageNet	ResNet50 (FL 3)	1.93	9.88	3.13	1.77	2.61	2.70	66.65
TinyImageNet	ResNet50 (LS 0.05)	15.73	6.29	3.02	7.02	7.18	7.56	60.64

Table 6: ECE % – Expected Calibration Error (lower is better), 15 bins, group 2

Dataset	Model	Before calibration	Hist-binning	Isotonic	T-scaling	V-scaling	V-scaling-b	M-scaling-b
CIFAR-10	DenseNet121	0.513	0.509	0.566	0.514	0.548	0.491	0.483
CIFAR-10	DenseNet161	0.646	0.536	0.534	0.629	0.531	0.527	0.536
CIFAR-10	DenseNet169	0.551	0.566	0.527	0.536	0.485	0.490	0.518
CIFAR-10	GoogLeNet	0.641	0.579	0.543	0.559	0.544	0.520	0.545
CIFAR-10	InceptionV3	0.596	0.573	0.543	0.598	0.543	0.573	0.553
CIFAR-10	MobileNetV2	0.638	0.500	0.502	0.543	0.572	0.574	0.546
CIFAR-10	ResNet18	0.649	0.578	0.570	0.634	0.590	0.538	0.581
CIFAR-10	ResNet34	0.714	0.549	0.549	0.671	0.584	0.566	0.570
CIFAR-10	ResNet50	0.596	0.523	0.522	0.555	0.556	0.511	0.530
CIFAR-10	VGG11_bn	0.633	0.579	0.517	0.635	0.620	0.506	0.523
CIFAR-10	VGG13_bn	0.563	0.536	0.443	0.572	0.510	0.488	0.461
CIFAR-10	VGG16_bn	0.542	0.617	0.478	0.548	0.550	0.477	0.518
CIFAR-10	VGG19_bn	0.578	0.526	0.443	0.514	0.531	0.460	0.495
CIFAR-100	MobileNetV2_x0_5	0.364	0.325	0.289	0.260	0.270	0.266	0.893
CIFAR-100	MobileNetV2_x1_0	0.337	0.295	0.266	0.264	0.262	0.254	0.815
CIFAR-100	MobileNetV2_x1_4	0.305	0.297	0.254	0.246	0.251	0.245	0.737
CIFAR-100	ResNet20	0.357	0.338	0.287	0.270	0.274	0.276	1.001
CIFAR-100	ResNet32	0.383	0.309	0.285	0.262	0.267	0.274	0.956
CIFAR-100	ResNet44	0.398	0.303	0.283	0.263	0.274	0.270	0.897
CIFAR-100	ResNet56	0.391	0.285	0.275	0.260	0.272	0.262	0.873
CIFAR-100	ShuffleNetV2_x0_5	0.379	0.312	0.288	0.261	0.272	0.276	0.999
CIFAR-100	ShuffleNetV2_x1_0	0.343	0.315	0.281	0.253	0.269	0.266	0.849
CIFAR-100	ShuffleNetV2_x1_5	0.302	0.290	0.259	0.259	0.265	0.255	0.773
CIFAR-100	ShuffleNetV2_x2_0	0.274	0.291	0.256	0.252	0.261	0.245	0.738
CIFAR-100	VGG11_bn	0.399	0.286	0.272	0.271	0.285	0.262	0.678
CIFAR-100	VGG13_bn	0.359	0.262	0.272	0.264	0.267	0.254	0.639
CIFAR-100	VGG16_bn	0.448	0.244	0.249	0.252	0.259	0.244	0.645
CIFAR-100	VGG19_bn	0.462	0.237	0.244	0.254	0.266	0.246	0.696
ImageNet	EfficientNet_b8	0.035	0.025	0.022	0.023	0.024	0.023	0.042
ImageNet	MobileNetV2_120d	0.036	0.034	0.030	0.030	0.030	0.030	0.080
ImageNet	RepVGG_b3	0.028	0.030	0.027	0.028	0.028	0.028	0.067
ImageNet	VGG19_bn	0.032	0.036	0.031	0.032	0.032	0.032	0.091

Table 7: cwECE % – Classwise Expected Calibration Error (lower is better), 15 bins, group 1

Dataset	Model	Before calibration	Hist-binning	Isotonic	T-scaling	V-scaling	V-scaling-b	M-scaling-b
CIFAR-10	DenseNet121 (CE)	0.948	0.478	0.530	0.548	0.485	0.455	0.461
CIFAR-10	DenseNet121 (FL 1)	0.755	0.487	0.376	0.462	0.430	0.416	0.540
CIFAR-10	DenseNet121 (FL 2)	0.514	0.488	0.424	0.462	0.419	0.431	0.428
CIFAR-10	DenseNet121 (FL 3)	0.524	0.489	0.474	0.532	0.508	0.483	0.517
CIFAR-10	DenseNet121 (LS 0.05)	0.576	0.376	0.446	0.514	0.410	0.317	0.392
CIFAR-10	ResNet110 (CE)	0.990	0.491	0.547	0.550	0.495	0.449	0.476
CIFAR-10	ResNet110 (FL 1)	0.804	0.483	0.404	0.517	0.511	0.449	0.458
CIFAR-10	ResNet110 (FL 2)	0.660	0.470	0.411	0.486	0.453	0.408	0.438
CIFAR-10	ResNet110 (FL 3)	0.505	0.436	0.400	0.500	0.417	0.418	0.425
CIFAR-10	ResNet110 (LS 0.05)	0.673	0.497	0.488	0.617	0.505	0.420	0.431
CIFAR-10	ResNet50 (CE)	0.941	0.469	0.493	0.524	0.454	0.435	0.428
CIFAR-10	ResNet50 (FL 1)	0.836	0.520	0.465	0.519	0.465	0.464	0.470
CIFAR-10	ResNet50 (FL 2)	0.625	0.506	0.457	0.511	0.485	0.465	0.455
CIFAR-10	ResNet50 (FL 3)	0.524	0.525	0.429	0.531	0.528	0.464	0.513
CIFAR-10	ResNet50 (LS 0.05)	0.766	0.520	0.455	0.634	0.525	0.459	0.440
CIFAR-10	Wide-ResNet-26-10 (CE)	0.699	0.399	0.388	0.440	0.404	0.371	0.382
CIFAR-10	Wide-ResNet-26-10 (FL 1)	0.611	0.442	0.399	0.412	0.402	0.400	0.375
CIFAR-10	Wide-ResNet-26-10 (FL 2)	0.479	0.443	0.436	0.462	0.428	0.437	0.429
CIFAR-10	Wide-ResNet-26-10 (FL 3)	0.523	0.401	0.377	0.452	0.400	0.373	0.407
CIFAR-10	Wide-ResNet-26-10 (LS 0.05)	0.869	0.417	0.424	0.502	0.458	0.400	0.415
CIFAR-100	DenseNet121 (CE)	0.458	0.210	0.239	0.258	0.252	0.226	0.688
CIFAR-100	DenseNet121 (FL 1)	0.364	0.231	0.249	0.267	0.261	0.237	0.695
CIFAR-100	DenseNet121 (FL 2)	0.280	0.278	0.241	0.256	0.252	0.239	0.694
CIFAR-100	DenseNet121 (FL 3)	0.254	0.283	0.248	0.252	0.258	0.244	0.698
CIFAR-100	DenseNet121 (LS 0.05)	0.315	0.223	0.238	0.252	0.223	0.206	0.668
CIFAR-100	ResNet110 (CE)	0.433	0.183	0.233	0.252	0.254	0.233	0.676
CIFAR-100	ResNet110 (FL 1)	0.372	0.231	0.243	0.262	0.257	0.229	0.669
CIFAR-100	ResNet110 (FL 2)	0.321	0.253	0.246	0.254	0.254	0.243	0.660
CIFAR-100	ResNet110 (FL 3)	0.281	0.257	0.245	0.258	0.258	0.241	0.671
CIFAR-100	ResNet110 (LS 0.05)	0.299	0.217	0.245	0.253	0.250	0.221	0.667
CIFAR-100	ResNet50 (CE)	0.412	0.215	0.250	0.259	0.259	0.240	0.683
CIFAR-100	ResNet50 (FL 1)	0.337	0.251	0.250	0.250	0.253	0.243	0.674
CIFAR-100	ResNet50 (FL 2)	0.282	0.272	0.251	0.250	0.244	0.234	0.692
CIFAR-100	ResNet50 (FL 3)	0.256	0.274	0.250	0.252	0.245	0.238	0.707
CIFAR-100	ResNet50 (LS 0.05)	0.271	0.222	0.239	0.258	0.243	0.225	0.640
CIFAR-100	Wide-ResNet-26-10 (CE)	0.372	0.198	0.229	0.230	0.241	0.219	0.645
CIFAR-100	Wide-ResNet-26-10 (FL 1)	0.264	0.238	0.229	0.223	0.219	0.210	0.624
CIFAR-100	Wide-ResNet-26-10 (FL 2)	0.218	0.245	0.211	0.216	0.215	0.208	0.611
CIFAR-100	Wide-ResNet-26-10 (FL 3)	0.226	0.260	0.216	0.228	0.220	0.215	0.596
CIFAR-100	Wide-ResNet-26-10 (LS 0.05)	0.239	0.222	0.229	0.240	0.238	0.219	0.608
TinyImageNet	ResNet50 (CE)	0.250	0.218	0.216	0.201	0.213	0.208	0.671
TinyImageNet	ResNet50 (FL 1)	0.218	0.226	0.199	0.205	0.216	0.212	0.684
TinyImageNet	ResNet50 (FL 2)	0.205	0.228	0.208	0.203	0.214	0.204	0.678
TinyImageNet	ResNet50 (FL 3)	0.203	0.227	0.202	0.204	0.217	0.209	0.677
TinyImageNet	ResNet50 (LS 0.05)	0.231	0.210	0.203	0.200	0.206	0.203	0.628

Table 8: cwECE % – Classwise Expected Calibration Error (lower is better), 15 bins, group 2

Dataset	Model	Before calibration	Hist-binning	Isotonic	T-scaling	V-scaling	V-scaling-b	M-scaling-b
CIFAR-10	DenseNet121	42.22	32.98	80.26	41.59	25.41	29.82	36.27
CIFAR-10	DenseNet161	25.30	38.11	16.86	27.21	24.37	26.92	34.27
CIFAR-10	DenseNet169	20.25	34.25	16.18	22.95	41.38	36.91	26.38
CIFAR-10	GoogLeNet	19.85	24.06	24.77	13.08	16.88	25.35	42.19
CIFAR-10	InceptionV3	31.42	80.60	17.31	31.74	20.06	33.00	28.17
CIFAR-10	MobileNetV2	33.59	68.23	25.32	24.74	32.21	74.59	27.27
CIFAR-10	ResNet18	34.79	28.21	17.80	28.45	76.02	24.15	24.30
CIFAR-10	ResNet34	23.94	42.79	18.42	24.47	31.98	25.98	21.92
CIFAR-10	ResNet50	26.73	41.10	19.27	24.68	24.24	16.52	31.25
CIFAR-10	VGG11_bn	23.38	16.46	16.86	23.40	18.33	16.37	25.19
CIFAR-10	VGG13_bn	33.53	25.74	14.47	36.17	40.39	25.12	23.99
CIFAR-10	VGG16_bn	43.19	34.06	19.88	43.57	26.82	22.98	20.03
CIFAR-10	VGG19_bn	35.49	33.63	18.37	22.27	36.65	24.40	19.50
CIFAR-100	MobileNetV2_x0_5	39.98	22.95	14.67	43.49	9.70	11.54	89.36
CIFAR-100	MobileNetV2_x1_0	28.71	25.03	17.36	9.74	7.37	9.69	77.00
CIFAR-100	MobileNetV2_x1_4	25.60	25.06	12.64	6.32	8.72	10.38	90.57
CIFAR-100	ResNet20	38.15	23.61	13.66	12.52	8.89	14.32	76.15
CIFAR-100	ResNet32	32.21	22.11	13.88	9.12	9.37	9.23	84.30
CIFAR-100	ResNet44	32.68	28.18	15.00	9.09	10.82	12.42	92.21
CIFAR-100	ResNet56	30.81	61.69	14.19	10.67	7.78	9.63	82.18
CIFAR-100	ShuffleNetV2_x0_5	23.82	21.63	12.26	8.51	7.89	8.38	76.58
CIFAR-100	ShuffleNetV2_x1_0	24.66	24.33	18.31	13.27	14.08	10.62	82.94
CIFAR-100	ShuffleNetV2_x1_5	24.47	24.70	14.58	17.98	13.47	12.31	71.59
CIFAR-100	ShuffleNetV2_x2_0	93.58	24.84	13.84	27.37	27.23	12.18	83.28
CIFAR-100	VGG11_bn	40.53	29.29	20.59	15.36	13.28	14.15	47.91
CIFAR-100	VGG13_bn	34.00	33.38	18.11	16.34	13.75	13.11	51.88
CIFAR-100	VGG16_bn	48.47	45.52	16.72	12.39	13.18	15.35	76.81
CIFAR-100	VGG19_bn	51.11	38.46	16.52	17.08	14.98	13.73	54.69
ImageNet	EfficientNet_b8	44.80	22.83	12.03	93.37	22.61	17.02	55.00
ImageNet	MobileNetV2_120d	12.31	18.22	6.16	3.75	5.92	5.65	63.64
ImageNet	RepVGG_b3	11.15	19.16	7.36	10.09	10.68	14.01	61.53
ImageNet	VGG19_bn	8.33	20.24	8.72	6.40	5.48	4.71	72.88

Table 9: MCE % – Maximum Calibration Error (lower is better), 15 bins, group 1

Dataset	Model	Before calibration	Hist-binning	Isotonic	T-scaling	V-scaling	V-scaling-b	M-scaling-b
CIFAR-10	DenseNet121 (CE)	46.58	53.58	23.62	22.26	29.52	23.21	67.72
CIFAR-10	DenseNet121 (FL 1)	36.54	37.23	26.98	29.38	31.21	70.77	22.20
CIFAR-10	DenseNet121 (FL 2)	27.80	35.64	10.22	66.85	29.08	28.61	29.06
CIFAR-10	DenseNet121 (FL 3)	77.08	38.19	38.07	76.59	74.49	19.89	23.57
CIFAR-10	DenseNet121 (LS 0.05)	55.74	56.99	80.80	70.26	57.18	66.81	40.70
CIFAR-10	ResNet110 (CE)	47.15	50.61	35.38	25.12	25.90	27.26	31.14
CIFAR-10	ResNet110 (FL 1)	73.35	61.93	26.03	49.35	19.64	42.96	29.91
CIFAR-10	ResNet110 (FL 2)	26.15	30.54	24.24	23.77	25.80	32.68	28.42
CIFAR-10	ResNet110 (FL 3)	25.15	30.68	29.37	38.39	30.89	69.55	30.64
CIFAR-10	ResNet110 (LS 0.05)	55.53	83.03	20.67	59.80	58.54	59.94	48.80
CIFAR-10	ResNet50 (CE)	42.08	55.72	22.08	20.49	32.80	18.27	31.52
CIFAR-10	ResNet50 (FL 1)	37.23	73.04	22.43	31.58	73.41	26.62	34.54
CIFAR-10	ResNet50 (FL 2)	25.00	41.04	74.60	67.95	76.43	29.61	32.46
CIFAR-10	ResNet50 (FL 3)	28.99	32.00	11.89	19.15	24.35	31.04	30.76
CIFAR-10	ResNet50 (LS 0.05)	50.21	45.06	21.05	74.74	51.06	76.52	43.41
CIFAR-10	Wide-ResNet-26-10 (CE)	48.03	63.54	25.41	30.04	30.41	31.41	32.78
CIFAR-10	Wide-ResNet-26-10 (FL 1)	26.49	48.07	18.55	75.41	24.17	31.02	21.96
CIFAR-10	Wide-ResNet-26-10 (FL 2)	33.49	74.05	23.92	31.05	29.04	24.23	37.53
CIFAR-10	Wide-ResNet-26-10 (FL 3)	28.18	19.14	18.52	69.02	31.10	17.94	29.90
CIFAR-10	Wide-ResNet-26-10 (LS 0.05)	39.10	36.02	19.03	31.45	71.21	36.22	42.35
CIFAR-100	DenseNet121 (CE)	54.14	29.97	21.75	28.70	12.36	12.84	77.88
CIFAR-100	DenseNet121 (FL 1)	35.37	36.84	17.62	16.51	14.52	14.35	86.25
CIFAR-100	DenseNet121 (FL 2)	26.13	24.50	15.21	12.86	14.74	15.88	82.62
CIFAR-100	DenseNet121 (FL 3)	14.76	23.33	11.81	12.16	13.74	9.81	76.96
CIFAR-100	DenseNet121 (LS 0.05)	46.99	30.43	22.79	60.42	12.61	11.28	75.69
CIFAR-100	ResNet110 (CE)	58.32	43.75	19.58	24.80	19.10	17.70	85.79
CIFAR-100	ResNet110 (FL 1)	38.23	41.78	20.14	18.67	20.87	17.51	70.51
CIFAR-100	ResNet110 (FL 2)	30.27	30.83	15.95	19.63	18.86	14.13	89.28
CIFAR-100	ResNet110 (FL 3)	25.44	23.25	16.91	21.06	16.78	15.19	69.21
CIFAR-100	ResNet110 (LS 0.05)	40.00	30.48	15.85	30.16	20.27	20.47	89.53
CIFAR-100	ResNet50 (CE)	47.19	47.37	20.20	16.26	20.44	22.76	83.57
CIFAR-100	ResNet50 (FL 1)	34.78	32.35	21.41	16.26	13.78	15.34	53.71
CIFAR-100	ResNet50 (FL 2)	23.83	25.69	14.62	14.00	15.24	16.00	91.02
CIFAR-100	ResNet50 (FL 3)	14.00	20.36	9.20	12.66	12.36	10.70	89.46
CIFAR-100	ResNet50 (LS 0.05)	31.28	29.37	94.39	23.55	21.02	18.71	69.93
CIFAR-100	Wide-ResNet-26-10 (CE)	55.83	46.57	21.84	15.99	14.89	14.20	83.06
CIFAR-100	Wide-ResNet-26-10 (FL 1)	27.40	30.07	16.22	12.96	14.48	13.07	72.31
CIFAR-100	Wide-ResNet-26-10 (FL 2)	16.16	27.35	11.15	12.62	13.02	26.94	88.77
CIFAR-100	Wide-ResNet-26-10 (FL 3)	9.90	24.61	13.33	12.65	16.52	44.60	80.98
CIFAR-100	Wide-ResNet-26-10 (LS 0.05)	26.84	32.39	20.92	27.45	24.19	18.73	75.74
TinyImageNet	ResNet50 (CE)	33.75	21.46	26.91	17.26	15.41	17.65	80.79
TinyImageNet	ResNet50 (FL 1)	18.63	14.14	17.73	9.08	12.43	17.18	78.34
TinyImageNet	ResNet50 (FL 2)	9.53	14.57	9.68	7.69	9.86	10.83	71.59
TinyImageNet	ResNet50 (FL 3)	6.39	14.29	10.00	6.21	7.30	11.51	77.58
TinyImageNet	ResNet50 (LS 0.05)	26.59	15.09	7.08	13.56	17.30	18.21	77.05

Table 10: MCE % – Maximum Calibration Error (lower is better), 15 bins, group 2

C Proper Scoring Rules

Dataset	Model	Before calibration	Hist-binning	Isotonic	T-scaling	V-scaling	V-scaling-b	M-scaling-b
CIFAR-10	DenseNet121	0.257	0.427	0.354	0.257	0.258	0.255	0.256
CIFAR-10	DenseNet161	0.261	0.495	0.285	0.262	0.255	0.253	0.281
CIFAR-10	DenseNet169	0.245	0.559	0.309	0.245	0.242	0.242	0.258
CIFAR-10	GoogleNet	0.246	0.290	0.300	0.241	0.241	0.239	0.235
CIFAR-10	InceptionV3	0.265	0.550	0.349	0.266	0.264	0.264	0.264
CIFAR-10	MobileNetV2	0.241	0.494	0.309	0.239	0.239	0.237	0.239
CIFAR-10	ResNet18	0.269	0.616	0.327	0.269	0.265	0.263	0.269
CIFAR-10	ResNet34	0.269	0.508	0.317	0.265	0.261	0.260	0.265
CIFAR-10	ResNet50	0.255	0.589	0.289	0.253	0.252	0.251	0.258
CIFAR-10	VGG11_bn	0.257	0.410	0.342	0.257	0.255	0.252	0.254
CIFAR-10	VGG13_bn	0.207	0.487	0.249	0.207	0.205	0.202	0.206
CIFAR-10	VGG16_bn	0.233	0.522	0.276	0.232	0.230	0.229	0.237
CIFAR-10	VGG19_bn	0.248	0.553	0.291	0.245	0.244	0.242	0.250
CIFAR-100	MobileNetV2_x0_5	1.210	4.128	1.738	1.066	1.073	1.083	15.290
CIFAR-100	MobileNetV2_x1_0	1.102	4.019	1.480	0.979	0.986	0.986	13.881
CIFAR-100	MobileNetV2_x1_4	0.997	3.823	1.499	0.908	0.911	0.909	12.531
CIFAR-100	ResNet20	1.267	4.445	1.771	1.155	1.161	1.164	17.232
CIFAR-100	ResNet32	1.370	4.573	1.762	1.148	1.155	1.162	16.467
CIFAR-100	ResNet44	1.358	4.350	1.656	1.097	1.104	1.110	15.459
CIFAR-100	ResNet56	1.340	3.933	1.711	1.069	1.076	1.075	15.020
CIFAR-100	ShuffleNetV2_x0_5	1.342	4.479	1.795	1.196	1.199	1.206	16.835
CIFAR-100	ShuffleNetV2_x1_0	1.200	4.205	1.760	1.089	1.098	1.103	14.203
CIFAR-100	ShuffleNetV2_x1_5	1.109	3.727	1.594	1.052	1.053	1.054	12.794
CIFAR-100	ShuffleNetV2_x2_0	1.018	3.610	1.613	0.992	0.999	0.997	12.425
CIFAR-100	VGG11_bn	1.541	3.978	1.840	1.259	1.275	1.270	4.707
CIFAR-100	VGG13_bn	1.320	3.361	1.642	1.106	1.118	1.117	4.230
CIFAR-100	VGG16_bn	1.677	3.162	1.584	1.142	1.148	1.144	5.757
CIFAR-100	VGG19_bn	1.836	3.034	1.621	1.158	1.162	1.158	7.711
ImageNet	EfficientNet_b8	0.656	2.778	1.432	0.572	0.581	0.664	5.554
ImageNet	MobileNetV2_120d	0.946	4.282	1.917	0.894	0.900	0.931	10.508
ImageNet	RepVGG_b3	0.823	3.751	1.795	0.815	0.811	0.871	9.225
ImageNet	VGG19_bn	1.034	4.892	2.100	1.017	1.021	1.040	13.665

Table 11: Negative Log-Likelihood (lower is better), group 1

Dataset	Model	Before calibration	Hist-binning	Isotonic	T-scaling	V-scaling	V-scaling-b	M-scaling-b
CIFAR-10	DenseNet121 (CE)	0.422	0.398	0.213	0.216	0.209	0.206	0.198
CIFAR-10	DenseNet121 (FL 1)	0.230	0.508	0.271	0.190	0.185	0.182	0.193
CIFAR-10	DenseNet121 (FL 2)	0.186	0.548	0.278	0.181	0.178	0.178	0.182
CIFAR-10	DenseNet121 (FL 3)	0.193	0.369	0.312	0.194	0.191	0.191	0.206
CIFAR-10	DenseNet121 (LS 0.05)	0.306	0.389	0.334	0.306	0.298	0.293	0.302
CIFAR-10	ResNet110 (CE)	0.512	0.454	0.227	0.230	0.224	0.222	0.228
CIFAR-10	ResNet110 (FL 1)	0.234	0.547	0.285	0.181	0.181	0.177	0.182
CIFAR-10	ResNet110 (FL 2)	0.195	0.477	0.261	0.179	0.177	0.174	0.176
CIFAR-10	ResNet110 (FL 3)	0.185	0.478	0.252	0.183	0.178	0.177	0.185
CIFAR-10	ResNet110 (LS 0.05)	0.301	0.434	0.302	0.301	0.294	0.289	0.290
CIFAR-10	ResNet50 (CE)	0.428	0.516	0.207	0.212	0.207	0.203	0.203
CIFAR-10	ResNet50 (FL 1)	0.253	0.604	0.246	0.193	0.187	0.184	0.188
CIFAR-10	ResNet50 (FL 2)	0.191	0.530	0.292	0.181	0.177	0.176	0.186
CIFAR-10	ResNet50 (FL 3)	0.190	0.485	0.237	0.188	0.186	0.185	0.199
CIFAR-10	ResNet50 (LS 0.05)	0.293	0.575	0.310	0.292	0.285	0.280	0.296
CIFAR-10	Wide-ResNet-26-10 (CE)	0.273	0.400	0.171	0.156	0.156	0.153	0.154
CIFAR-10	Wide-ResNet-26-10 (FL 1)	0.181	0.454	0.209	0.158	0.158	0.157	0.162
CIFAR-10	Wide-ResNet-26-10 (FL 2)	0.161	0.447	0.244	0.159	0.157	0.156	0.160
CIFAR-10	Wide-ResNet-26-10 (FL 3)	0.158	0.334	0.206	0.157	0.152	0.151	0.161
CIFAR-10	Wide-ResNet-26-10 (LS 0.05)	0.224	0.389	0.279	0.217	0.211	0.207	0.230
CIFAR-100	DenseNet121 (CE)	2.063	2.325	1.564	1.200	1.183	1.173	11.759
CIFAR-100	DenseNet121 (FL 1)	1.188	3.153	1.582	1.031	1.012	1.006	11.888
CIFAR-100	DenseNet121 (FL 2)	0.948	3.645	1.437	0.928	0.917	0.913	11.761
CIFAR-100	DenseNet121 (FL 3)	0.903	3.609	1.484	0.902	0.903	0.905	11.792
CIFAR-100	DenseNet121 (LS 0.05)	1.435	2.492	1.899	1.375	1.356	1.349	11.259
CIFAR-100	ResNet110 (CE)	1.843	2.391	1.382	1.074	1.076	1.070	11.560
CIFAR-100	ResNet110 (FL 1)	1.165	2.900	1.493	0.969	0.964	0.962	11.421
CIFAR-100	ResNet110 (FL 2)	1.006	3.352	1.507	0.942	0.937	0.935	11.200
CIFAR-100	ResNet110 (FL 3)	0.941	3.254	1.507	0.922	0.918	0.913	11.475
CIFAR-100	ResNet110 (LS 0.05)	1.363	2.603	1.847	1.325	1.325	1.313	11.344
CIFAR-100	ResNet50 (CE)	1.582	2.785	1.538	1.089	1.092	1.084	11.625
CIFAR-100	ResNet50 (FL 1)	1.094	3.426	1.625	0.969	0.969	0.965	11.530
CIFAR-100	ResNet50 (FL 2)	0.951	3.301	1.436	0.924	0.920	0.920	11.816
CIFAR-100	ResNet50 (FL 3)	0.897	3.491	1.514	0.893	0.887	0.885	12.042
CIFAR-100	ResNet50 (LS 0.05)	1.230	3.014	1.727	1.220	1.216	1.205	10.760
CIFAR-100	Wide-ResNet-26-10 (CE)	1.437	2.430	1.354	0.979	0.990	0.982	10.962
CIFAR-100	Wide-ResNet-26-10 (FL 1)	0.898	2.725	1.293	0.846	0.845	0.844	10.631
CIFAR-100	Wide-ResNet-26-10 (FL 2)	0.780	3.031	1.245	0.780	0.779	0.780	10.419
CIFAR-100	Wide-ResNet-26-10 (FL 3)	0.759	3.206	1.327	0.755	0.752	0.755	10.240
CIFAR-100	Wide-ResNet-26-10 (LS 0.05)	1.109	2.754	1.549	1.109	1.106	1.095	10.395
TinyImageNet	ResNet50 (CE)	2.325	6.905	3.478	2.199	2.213	2.214	21.369
TinyImageNet	ResNet50 (FL 1)	2.180	6.833	3.411	2.160	2.170	2.167	22.083
TinyImageNet	ResNet50 (FL 2)	2.033	6.626	3.158	2.032	2.048	2.042	21.973
TinyImageNet	ResNet50 (FL 3)	2.038	6.768	3.004	2.036	2.057	2.047	21.756
TinyImageNet	ResNet50 (LS 0.05)	2.334	5.121	3.108	2.129	2.142	2.141	18.609

Table 12: Negative Log-Likelihood (lower is better), group 2

Dataset	Model	Before calibration	Hist-binning	Isotonic	T-scaling	V-scaling	V-scaling-b	M-scaling-b
CIFAR-10	DenseNet121	0.102	0.106	0.099	0.102	0.102	0.102	0.101
CIFAR-10	DenseNet161	0.102	0.107	0.098	0.103	0.101	0.101	0.104
CIFAR-10	DenseNet169	0.098	0.106	0.095	0.099	0.098	0.098	0.100
CIFAR-10	GoogLeNet	0.109	0.112	0.109	0.109	0.110	0.109	0.110
CIFAR-10	InceptionV3	0.108	0.115	0.105	0.109	0.109	0.108	0.109
CIFAR-10	MobileNetV2	0.102	0.106	0.099	0.103	0.103	0.102	0.103
CIFAR-10	ResNet18	0.117	0.124	0.113	0.116	0.115	0.115	0.117
CIFAR-10	ResNet34	0.113	0.116	0.106	0.111	0.110	0.110	0.111
CIFAR-10	ResNet50	0.107	0.112	0.102	0.106	0.105	0.105	0.106
CIFAR-10	VGG11_bn	0.118	0.122	0.115	0.118	0.118	0.117	0.118
CIFAR-10	VGG13_bn	0.092	0.102	0.091	0.093	0.093	0.092	0.094
CIFAR-10	VGG16_bn	0.100	0.108	0.097	0.100	0.099	0.099	0.101
CIFAR-10	VGG19_bn	0.102	0.109	0.098	0.101	0.101	0.100	0.102
CIFAR-100	MobileNetV2_x0_5	0.431	0.469	0.413	0.404	0.406	0.408	0.892
CIFAR-100	MobileNetV2_x1_0	0.387	0.431	0.373	0.365	0.367	0.368	0.814
CIFAR-100	MobileNetV2_x1_4	0.352	0.402	0.341	0.336	0.337	0.337	0.736
CIFAR-100	ResNet20	0.459	0.511	0.448	0.438	0.440	0.441	1.001
CIFAR-100	ResNet32	0.453	0.493	0.431	0.420	0.423	0.424	0.956
CIFAR-100	ResNet44	0.441	0.475	0.411	0.403	0.405	0.406	0.897
CIFAR-100	ResNet56	0.429	0.451	0.397	0.392	0.394	0.395	0.873
CIFAR-100	ShuffleNetV2_x0_5	0.468	0.510	0.450	0.442	0.443	0.445	0.996
CIFAR-100	ShuffleNetV2_x1_0	0.413	0.451	0.401	0.392	0.395	0.396	0.847
CIFAR-100	ShuffleNetV2_x1_5	0.384	0.426	0.377	0.373	0.373	0.374	0.770
CIFAR-100	ShuffleNetV2_x2_0	0.359	0.408	0.354	0.352	0.353	0.353	0.736
CIFAR-100	VGG11_bn	0.455	0.473	0.424	0.415	0.419	0.419	0.673
CIFAR-100	VGG13_bn	0.406	0.425	0.381	0.373	0.375	0.375	0.629
CIFAR-100	VGG16_bn	0.450	0.439	0.386	0.382	0.383	0.382	0.633
CIFAR-100	VGG19_bn	0.456	0.436	0.380	0.379	0.378	0.377	0.672
ImageNet	EfficientNet_b8	0.222	0.251	0.217	0.215	0.217	0.219	0.407
ImageNet	MobileNetV2_120d	0.323	0.379	0.324	0.314	0.319	0.322	0.776
ImageNet	RepVGG_b3	0.283	0.332	0.286	0.282	0.285	0.289	0.655
ImageNet	VGG19_bn	0.354	0.423	0.363	0.353	0.358	0.361	0.900

Table 13: Brier Score (lower is better), group 1

Dataset	Model	Before calibration	Hist-binning	Isotonic	T-scaling	V-scaling	V-scaling-b	M-scaling-b
CIFAR-10	DenseNet121 (CE)	0.094	0.094	0.081	0.084	0.082	0.082	0.082
CIFAR-10	DenseNet121 (FL 1)	0.086	0.092	0.079	0.081	0.080	0.080	0.084
CIFAR-10	DenseNet121 (FL 2)	0.081	0.089	0.079	0.080	0.079	0.079	0.080
CIFAR-10	DenseNet121 (FL 3)	0.089	0.091	0.088	0.089	0.088	0.088	0.090
CIFAR-10	DenseNet121 (LS 0.05)	0.102	0.102	0.091	0.103	0.102	0.101	0.100
CIFAR-10	ResNet110 (CE)	0.097	0.098	0.086	0.087	0.086	0.086	0.086
CIFAR-10	ResNet110 (FL 1)	0.086	0.088	0.078	0.079	0.078	0.078	0.078
CIFAR-10	ResNet110 (FL 2)	0.082	0.087	0.079	0.079	0.078	0.078	0.079
CIFAR-10	ResNet110 (FL 3)	0.083	0.088	0.081	0.082	0.079	0.079	0.082
CIFAR-10	ResNet110 (LS 0.05)	0.103	0.103	0.092	0.103	0.102	0.101	0.099
CIFAR-10	ResNet50 (CE)	0.093	0.098	0.084	0.085	0.084	0.083	0.084
CIFAR-10	ResNet50 (FL 1)	0.091	0.098	0.083	0.084	0.083	0.083	0.083
CIFAR-10	ResNet50 (FL 2)	0.083	0.091	0.080	0.081	0.079	0.079	0.081
CIFAR-10	ResNet50 (FL 3)	0.085	0.092	0.084	0.084	0.084	0.084	0.088
CIFAR-10	ResNet50 (LS 0.05)	0.102	0.106	0.094	0.102	0.101	0.101	0.099
CIFAR-10	Wide-ResNet-26-10 (CE)	0.069	0.070	0.061	0.061	0.061	0.061	0.061
CIFAR-10	Wide-ResNet-26-10 (FL 1)	0.070	0.077	0.067	0.067	0.068	0.068	0.067
CIFAR-10	Wide-ResNet-26-10 (FL 2)	0.071	0.078	0.068	0.070	0.071	0.070	0.071
CIFAR-10	Wide-ResNet-26-10 (FL 3)	0.068	0.072	0.067	0.069	0.068	0.067	0.069
CIFAR-10	Wide-ResNet-26-10 (LS 0.05)	0.076	0.078	0.072	0.077	0.076	0.076	0.077
CIFAR-100	DenseNet121 (CE)	0.446	0.413	0.368	0.372	0.364	0.364	0.687
CIFAR-100	DenseNet121 (FL 1)	0.385	0.394	0.351	0.354	0.348	0.347	0.694
CIFAR-100	DenseNet121 (FL 2)	0.348	0.389	0.336	0.339	0.336	0.336	0.693
CIFAR-100	DenseNet121 (FL 3)	0.336	0.391	0.337	0.336	0.336	0.336	0.697
CIFAR-100	DenseNet121 (LS 0.05)	0.406	0.405	0.378	0.387	0.378	0.378	0.667
CIFAR-100	ResNet110 (CE)	0.421	0.393	0.347	0.349	0.346	0.345	0.675
CIFAR-100	ResNet110 (FL 1)	0.375	0.384	0.333	0.336	0.333	0.332	0.669
CIFAR-100	ResNet110 (FL 2)	0.358	0.387	0.334	0.339	0.337	0.336	0.658
CIFAR-100	ResNet110 (FL 3)	0.346	0.379	0.331	0.337	0.334	0.333	0.670
CIFAR-100	ResNet110 (LS 0.05)	0.386	0.401	0.366	0.372	0.372	0.371	0.665
CIFAR-100	ResNet50 (CE)	0.411	0.406	0.355	0.353	0.353	0.353	0.682
CIFAR-100	ResNet50 (FL 1)	0.365	0.393	0.341	0.337	0.335	0.334	0.673
CIFAR-100	ResNet50 (FL 2)	0.346	0.388	0.337	0.337	0.335	0.335	0.691
CIFAR-100	ResNet50 (FL 3)	0.331	0.382	0.332	0.329	0.328	0.328	0.706
CIFAR-100	ResNet50 (LS 0.05)	0.365	0.390	0.351	0.359	0.357	0.356	0.639
CIFAR-100	Wide-ResNet-26-10 (CE)	0.365	0.364	0.316	0.310	0.312	0.311	0.645
CIFAR-100	Wide-ResNet-26-10 (FL 1)	0.304	0.337	0.294	0.291	0.290	0.290	0.623
CIFAR-100	Wide-ResNet-26-10 (FL 2)	0.287	0.331	0.284	0.286	0.284	0.284	0.611
CIFAR-100	Wide-ResNet-26-10 (FL 3)	0.281	0.336	0.280	0.283	0.281	0.281	0.596
CIFAR-100	Wide-ResNet-26-10 (LS 0.05)	0.326	0.363	0.317	0.325	0.323	0.322	0.607
TinyImageNet	ResNet50 (CE)	0.677	0.720	0.661	0.646	0.652	0.654	1.324
TinyImageNet	ResNet50 (FL 1)	0.648	0.714	0.650	0.641	0.645	0.646	1.352
TinyImageNet	ResNet50 (FL 2)	0.620	0.688	0.630	0.620	0.627	0.627	1.343
TinyImageNet	ResNet50 (FL 3)	0.624	0.707	0.634	0.623	0.631	0.631	1.340
TinyImageNet	ResNet50 (LS 0.05)	0.645	0.682	0.617	0.613	0.620	0.621	1.229

Table 14: Brier Score (lower is better), group 2